Ultrasonic measurement of density of liquids

Article *in* The Journal of the Acoustical Society of America · January 1995

DOI: 10.1121/1.412320

5 authors, including:

Julio Cezar Adamowski
University of São Paulo
130 PUBLICATIONS **667** CITATIONS
SEE PROFILE

Flávio Buiochi
University of São Paulo
85 PUBLICATIONS **445** CITATIONS
SEE PROFILE

Claudio Simon
Philips
19 PUBLICATIONS **590** CITATIONS
SEE PROFILE

Emílio C. Nelli Silva
University of São Paulo
34 PUBLICATIONS **576** CITATIONS
SEE PROFILE

Ultrasonic measurement of density of liquids

Julio C. Adamowski,[a] Flávio Buiochi, Claudio Simon, and Emílio C. N. Silva
Department of Mechanical Engineering, Universidade de São Paulo, CxP 8174, 01065-970, São Paulo SP, Brazil

Rubens A. Sigelmann[b]
Department of Electrical Engineering, FT-10, University of Washington, Seattle, Washington 91195

(Received 10 February 1994; accepted for publication 11 August 1994)

This paper presents two methods to measure the density of liquids based on the measurement of the reflection coefficient and propagation velocity, using a novel double-element transducer. The measurements can be made in liquids, stationary or in motion. The main factors that affect the precision of the measurements are analyzed. The effect of acoustic diffraction is eliminated by using the double-element transducer, where the receiver is somewhat larger in diameter than the emitter. The effect of short- and long-term stability of the electronics and piezoelectric ceramics employed in the system is also eliminated. A system was implemented and measurements of several liquids, stationary and in motion, were conducted.

PACS numbers: 43.58.Bh, 43.20.Ye, 43.35.Yb

INTRODUCTION

The density ρ of a Newtonian liquid is obtained from the measurement of the characteristic (specific) acoustic impedance Z and the propagation velocity c through the relation $Z=\rho c$. The specific acoustic impedance Z is calculated from the measurement of the reflection or transmission coefficients. Hale[1] describes an ultrasonic method based on the transmission coefficient. He uses ultrasonic pulses propagating between receiving and transmitting transducers. Hale's implementation suffers limitations resulting from neglecting attenuation and from the need of calibrating the apparatus with a liquid of known properties. McClements and Fairley[2] attempt to circumvent the problems encountered by Hale, using a buffer rod of polymethyl-methacrylate and only one transducer operating in the pulse-echo mode.

The methods discussed above are highly dependent on the stability of the electronics and components. This requires frequent and careful calibrations. A method proposed by Papadakis[3–5] to measure the attenuation coefficient in solids resolves the problem of stability by using three reflected pulses. These pulses come from the interfaces: known material/sample and sample/air. In this method, the results are independent of the amplitude of the emitted pulse and of the attenuation in the buffer rod. Variations of this method, with an additional scheme to measure the propagation velocity, is implemented in a United States Patent[6] to measure the density of liquid fuels.

In the methods already discussed, the acoustic diffraction plays an important role in the accuracy of the measurement. This requires further mathematical corrections. An additional problem results from the fact that these corrections depend on the wavelength in the material to be tested. The diffraction effect is particularly severe in methods that use multiple reflections.

This article analyzes two methods to measure the reflection coefficients discussing the main factors that influence the accuracy of these methods (Sec. I). Then a study on accurate measurements of time delay between pulses, using cross-correlation, is presented (Sec. II) in order to obtain the propagation velocity in the liquid sample. The influence of the effect of frequency-dependent attenuation is also discussed. Section III shows how to calculate the liquid density given the reflection coefficients and the propagation velocity.

A good physical understanding of the structure of the acoustical field is provided by considering the plane and edge waves radiated by a transducer. A circular source radiates a plane wave into the geometrical region straight ahead of the source, together with a spreading edge wave from the periphery of the source.[7] It is clear that diffraction effects can be considered to be caused by the edge wave component of the field. It can be shown from the radiation theory that an infinite-plane receiver with uniform sensitivity is a plane-wave filter for the direction normal to the plane.[8] In the spatial integration of the field performed by an infinite-plane receiver the contributions made by the edge waves sum to zero, yielding a plane-wave-only measurement.[9] In practice, an infinite-plane receiver is modeled by using a PVDF (polyvinylidene fluoride) thin-film receiver, sufficiently large to intercept the entire propagating pulse and electroded throughout its entire extent. In this work a large-aperture PVDF receiver is used together with a piezoelectric ceramic emitter, resulting in a double-element transducer. The details of its construction are presented in Sec. IV. Two types of measuring cells employing this transducer were used to measure the density of stationary and flowing liquids (Sec. V). In Sec. VI, the laboratory setup used in the experiments is presented, while Sec. VII describes experiments conducted in water, both stationary and in motion. Castor oil, which has a very high attenuation, and ethanol, which has a lower density, were chosen to include the range of liquid properties

[a]E-mail: jcadamow@fox.cce.usp.br
[b]Visiting Professor at Universidade de São Paulo from March to August 1993.

 0001-4966/95/97(1)/354/8/$6.00

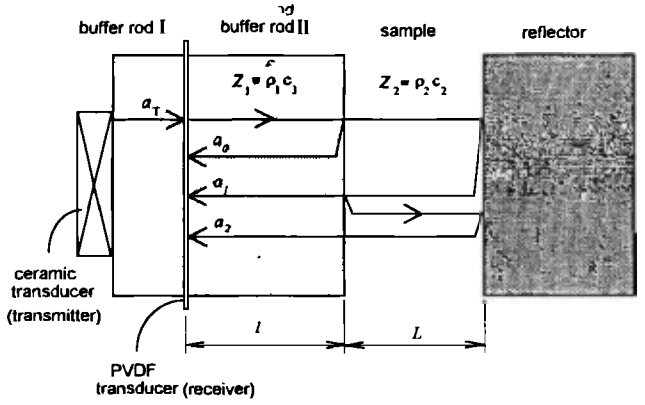

FIG. 1. Schematic diagram of the signals of interest in the density measurement. Although the pulses a_0, a_1, and a_2 continue propagating on buffer rod I, suffering reflection at the ceramic transducer interface and returning to the PVDF layer, they are not represented in the figure as they are not used in the measurements.

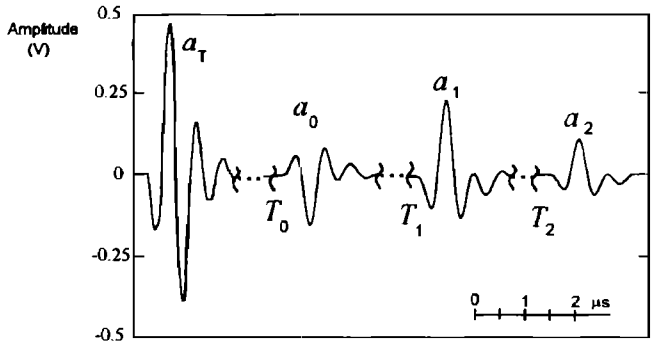

FIG. 2. Signals observed in the measurement (other signals are not represented).

that can be found in practice. An error analysis of the density measurement is also discussed. The conclusion is presented in Sec. VIII.

In Appendix A, the imaginary part of the specific acoustic impedance is calculated. In Appendix B, it is proved that the measurement of the propagation time between two echoes by cross correlation is not affected by attenuation.

I. MEASUREMENT OF THE REFLECTION COEFFICIENT

Considering plane-wave propagation and the unidimensional model, the reflection coefficient at the interface between two media of different characteristic acoustic impedance for normal incidence is given by

$$R_{12}=\frac{Z_2-Z_1}{Z_2+Z_1}, \tag{1}$$

where Z_1 and Z_2 are the characteristic acoustic impedances of media 1 and 2, respectively.

The basic components employed in the measurement of the reflection coefficient are shown in Fig. 1. The *double-element transducer* (DET) consists of a transmitter transducer made with a piezoelectric ceramic and a PVDF membrane that performs as a receiver transducer. These two elements are mounted in a buffer rod, as shown in Fig. 1. There are two methods of utilizing the DET to measure the reflection coefficient: The first method will be called the *multiple reflection method* (MRM) and the second one the *relative reflection method* (RRM).

The MRM is illustrated in Fig. 1. In this configuration, the sample is placed between the DET and a metal reflector. This figure shows the transmitted pulse a_T and three reflected pulses a_0, a_1, and a_2 which are used to calculate the reflection coefficient. These are the pulses as received by the PVDF transducer (Fig. 2). In the strict sense, to obtain the reflection coefficient, the Fourier transform of the pulses a_T, a_0, a_1, and a_2 must be calculated, and then at a particular frequency of the spectrum of each pulse, the magnitude value must be selected. It is assumed that A_T, A_0, A_1, and A_2 are such values, being associated the phase sign of the pulses a_T, a_0, a_1, and a_2. These values are related by the following expressions:

$$\begin{aligned} A_0&=A_T R_{12} e^{-2\alpha_1(f_1)l}, \\ A_1&=A_T T_{12} R_{23} T_{21} e^{-2\alpha_1(f_1)l} e^{-2\alpha_2(f_1)L}, \\ A_2&=A_T T_{12} R_{23} R_{21} R_{23} T_{21} e^{-2\alpha_1(f_1)l} e^{-4\alpha_2(f_1)L}, \end{aligned} \tag{2}$$

where R_{mn} is the reflection coefficient at the interface between media m and n, T_{mn} the transmission coefficient at the same interface, l the buffer rod II length, L the sample length, and $\alpha_1(f_1)$ and $\alpha_2(f_1)$ the attenuation coefficients (at a particular frequency f_1) in buffer rod II and in the liquid sample, respectively. After some calculation the following expression for the reflection coefficient R_{12} is obtained:

$$R_{12}=\left[\sqrt{\frac{A_0 A_2}{A_0 A_2 - A_1^2}}\right]_{f=f_1}. \tag{3}$$

The square brackets are used to emphasize that the values are obtained from the spectra at a particular frequency f_1. When the characteristic acoustic impedance of the buffer rod Z_1 is larger than the characteristic acoustic impedance Z_2 of the liquid sample, it must be noted that a_0 has an inverted phase with respect to a_T, a_1, and a_2 (Fig. 2). Since A_0 and A_2 are of opposite sign, the product $A_0 A_2$ is negative so the value inside the square root is positive. For the same reason, the negative value of the square root in Eq. (3) should be chosen.

The RRM is similar to the method proposed by McClements and Fairley[2] in that multiple reflections are not used to calculate the reflection coefficient. To eliminate the problems with equipment drift found in McClements' method, RRM employs a normalization with respect to A_T. A first measurement is performed without liquid in the sample chamber. The transmitted pulse as it propagates through the PVDF membrane generates the pulse $A_T(t_1)$ at the time t_1. The pulse is reflected at the interface buffer rod/air and returns to the PVDF membrane to generate the pulse $A_{\text{air}}(t_1+\tau_1)$, where τ_1 is a delay time. A second measurement is performed at the time t_2 with the liquid sample in the chamber and another pair of pulses $A_T(t_2)$ and $A_0(t_2+\tau_2)$, where τ_2 is a delay time obtained in the same way as the first measurement. This measurement may be repeated several times without having to repeat the first mea-

surement, provided that the temperature remains constant. These measurements are Fourier transforms, as in the MRM. The reflection coefficient for this method is

$$R_{12}=\left[\frac{A_0(t_2+\tau_2)/A_T(t_2)}{A_{\text{air}}(t_1+\tau_1)/A_T(t_1)}\right]_{f=f_1}. \tag{4}$$

The calculations of R_{12} [Eq. (1)] presumes that the characteristic acoustic impedance is real. For viscous liquids the characteristic acoustic impedance is complex. However, in the range of viscosity and frequency considered in this paper, the imaginary component of the characteristic acoustic impedance is negligible. This is discussed in Appendix A.

II. MEASUREMENT OF THE PROPAGATION VELOCITY

The basic technique of measurement of the propagation velocity consists of the measurement of the time T, the interval between two echoes from two interfaces in the liquid sample. As shown in Fig. 1, these intervals of time could be between echoes a_0 and a_1, or a_1 and a_2. Also, an accurate measurement of the distance L between these two interfaces is required. The propagation velocity c_2 is given by $c_2=2L/T$.

The main problem to determine the time interval stems from defining the beginning of the echoes. The technique of cross-correlation improves considerably this determination. This cross-correlation is calculated using the MATLAB™ software package. The echoes a_0, a_1, and a_2 must be digitized and transferred as data to the MATLAB™ software. In order to obtain better resolution, the echoes a_0, a_1, and a_2 are gated at T_0, T_1, and T_2 (Fig. 2). The times T_0, T_1, and T_2 are adjusted with an accuracy of ±500 ps ±0.002% of the reading (oscilloscope HP 54112D). The cross correlation of two time signals is given by

$$\gamma_{a_i a_j}(\tau)=\int_{-\infty}^{\infty} a_i(t)a_j(t+\tau)dt, \tag{5}$$

where $a_i(t)$ is the first echo and $a_j(t)$ the second echo. For the MRM, $i=0$ and $j=1$, or $i=1$ and $j=2$. For the RRM, $i=0$ and $j=1$. An example of a cross-correlogram of signals a_0 and a_1 is presented in Fig. 3. The first and second echoes have approximately the same shape, but the second is delayed by a time T. The echo $a_i(t)$ is gated at a starting time T_i, whereas $a_j(t)$ is gated at a starting time T_j. When the operation represented in Eq. (5) is performed, its absolute maximum value occurs at $\tau=T_{ij}$. The total time delay T is given by

$$T=T_j-T_i+T_{ij}. \tag{6}$$

The procedure just discussed may be applied to obtain the delay between the echoes a_T and a_0, which is used to determine the propagation velocity c_1 in the buffer rod.

All the discussions have so far ignored the effects of attenuation. It should be emphasized again that the measurement of the reflection coefficient, since it is performed at a particular frequency of the spectrum, is not affected by the attenuation. However, the same is not obvious for the measurement of the propagation velocity. When the attenuation in the liquid sample is a function of the frequency, as the pulse propagates through the liquid, in general, its shape changes. It is shown in Appendix B that the cross-correlation method is not affected by attenuation.

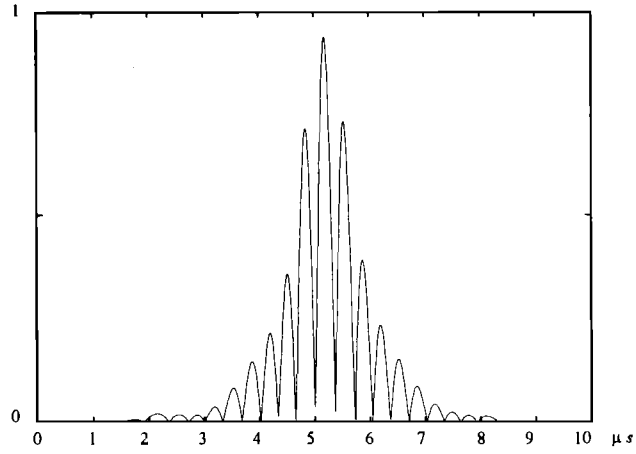

FIG. 3. Absolute values of the cross-correlation of signals a_0 and a_1, gated at T_0 and T_1. In this case the absolute maximum value occurs at $\tau=5.20$ μs (calculated by the software).

III. DENSITY MEASUREMENT

The liquid characteristic acoustic impedance Z_2 is obtained by rearranging Eq. (1): $Z_2=Z_1(1+R_{12})/(1-R_{12})$, where the reflection coefficient R_{12} may be calculated by Eq. (3) (MRM) or Eq. (4) (RRM), and Z_1 is the buffer rod impedance which is $Z_1=\rho_1 c_1$. The density ρ_1 is known and the propagation velocity c_1 is obtained by the method described in the previous section, using the pulses a_T and a_0.

The liquid density ρ_2 is calculated by $\rho_2=Z_2/c_2$, where the propagation velocity c_2 is measured as described above. Therefore

$$\rho_2=\frac{\rho_1 c_1(1+R_{12})}{c_2(1-R_{12})}. \tag{7}$$

A. Flowing liquids

The transmission and reflection coefficients of an acoustic wave that matches an interface with a flowing liquid layer are affected by the layer velocity. This influence depends mainly on the wave incidence angle. For an angle of incidence normal to the liquid layer velocity, the transmission and reflection coefficients are independent of the layer velocity.[10] So, if the incidence is normal, it may be expected that the density measurement results will not be affected in the case of flowing liquids.

IV. CONSTRUCTION OF THE DOUBLE-ELEMENT TRANSDUCER (DET)

The transducer described below has a solid medium separating the transmitter and the receiver, which are mounted in the same assembly. This particular construction has been previously proposed by Habeger and Wink[11] just to separate the transmitted and received electrical pulses. Adamowski,[12] on the other hand, used the same assembly in

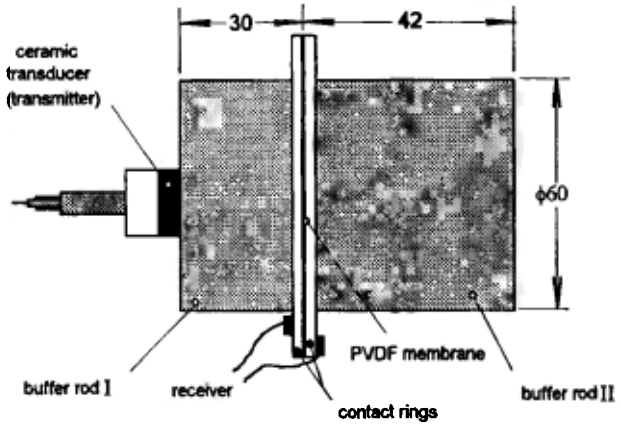

FIG. 4. Mechanical drawing of the double-element transducer (DET).

order to avoid the acoustic diffraction effects on the received signals and to eliminate short- and long-term stability of the electronics and piezoelectric ceramics.

Figure 4 shows a schematic drawing of the DET. The transmitter is a commercially available ceramic transducer (KB-Aerotech, medical purpose, broadband, central frequency 1.6 MHz, diameter 19 mm, nonfocused) and the receiver is a 52-μm-thick PVDF membrane with aluminum electrodes. One side of the PVDF membrane is bonded to buffer rod I and the other side is bonded to buffer rod II, both with a thin adhesive layer. Both buffer rods are made of polymethyl-methacrylate (PMMA), whose impedance approximately matches the membrane, reducing reflections at the interfaces of these media. This material is transparent, allowing the visualization of the bonding quality. The 80-mm-diam membrane is slightly larger than the 60-mm-diam buffer rods, so that a ring remains external to the assembly. Each electrode is electrically connected to the corresponding terminal by contact rings. This assembly, membrane (receiver) between two solids (buffer rods), provides a compact and stiff mounting of the DET.

The effective diameter of the receptor (60 mm) must be chosen in order to intercept the entire ultrasonic field produced by the transmitter and the echo pulses a_0, a_1, and a_2. In the worst case (a_2) the pulse propagates through a distance corresponding to buffer rod I plus twice buffer rod II plus 4× the sample length. In other words, the buffer rod diameter should be large enough to avoid reflection of the ultrasonic beam on the sidewalls. Buffer rod II length must be chosen so that echo superposition is avoided. The buffer rod faces are parallel in order to provide normal incidence, and smooth to prevent surface scattering.

V. MEASUREMENT CELLS

The density measurement cell for stationary liquids is shown schematically in Fig. 5. All the surfaces are maintained parallel by a monobloc construction. The central cavity contains the liquid sample and the through-hole permits perfect alignment between the DET and the reflector. A stainless-steel rod is used as the reflector. The rod is long enough to prevent internal reflections from interfering with the measurements.

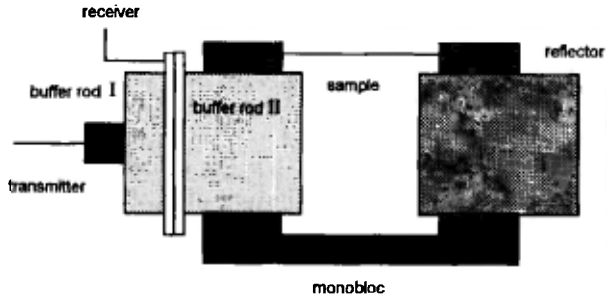

FIG. 5. Schematic drawing of the measurement cell for stationary liquids.

The cell used to measure the density of flowing liquids (Fig. 6) is installed in a hydraulic pipeline. The measurement cell was adapted in a PMMA rectangular section pipe (100×25 mm), so that the flow can be easily visualized. The DET and the reflector are positioned perpendicular to the flow, at opposite sides of the pipe transversal section. The sample length L may be adjusted by introducing the reflector rod into the pipe. Due to the pressure inside the pipe, it is necessary to use structural reinforcement in order to keep constant the sample length between the interface of the DET and the reflector.

VI. DESCRIPTION OF THE ELECTRONIC EQUIPMENT

Figure 7 presents a block diagram of the electronic instrumentation used throughout the experiments. The transducer is driven either by a short pulse or by a sinusoidal burst (one or more cycles). The first is generated by an ultrasonic analyzer (Panametrics model 5052UA), which allows variable control of the pulse energy, damping, and repetition rate. The burst is generated by a function generator (EMG model TR-0467) in conjunction with a rf power amplifier (ENI model 411LA, +40 dB).

The signals received by the PVDF membrane are amplified up to +40 dB by the ultrasonic analyzer. The signals are then acquired by a digital oscilloscope (Hewlett Packard model 54112D, 400 M sample/s, 8-bit resolution in average mode). It is possible to program several acquisition parameters, such as delay time, sensitivity, and sampling rate, so

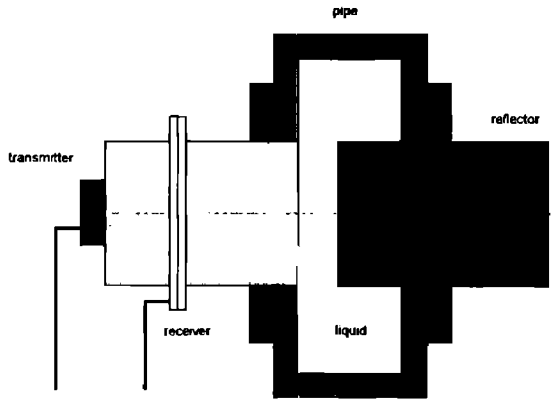

FIG. 6. Measurement cell for flowing liquids.

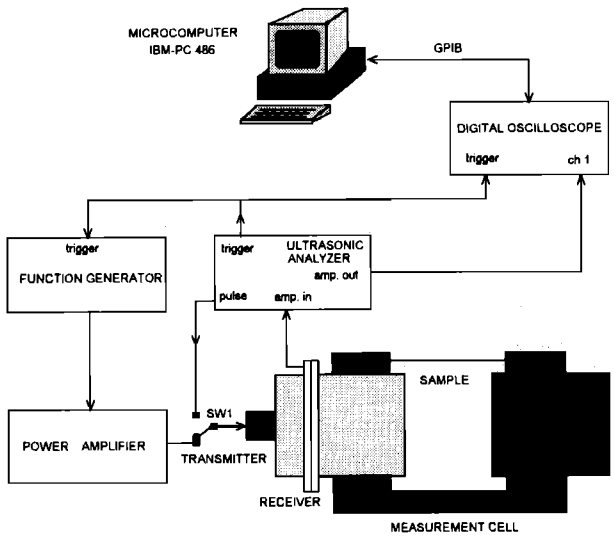

FIG. 7. Schematic of the experimental apparatus.

that each echo may be acquired independently. The averaging mode (1/64 weight), with a 100-M sample/s rate was used.

The oscilloscope is connected to an IBM-PC486 compatible microcomputer via an IEEE-488 interface (GPIB). This interface allows programming of the oscilloscope as well as transfer of data to the computer. The MATLAB™ software environment is used to digitally process the data.

VII. EXPERIMENTAL RESULTS

The experiments were conducted using the apparatus illustrated in Fig. 7. All the results presented were obtained with a one-cycle 1.6-MHz sinusoidal burst excitation pulse. Experiments with short pulses led to similar results. The temperature was measured with a 0.5 °C accuracy thermometer.

A. Density measurement of stationary liquids

Table I presents density values of the liquid samples measured with a 100-ml pycnometer. The distance between buffer rod II and the reflector was measured considering the propagation velocity in distilled water, being $L=11.50$ mm (Fig. 1). The buffer rod II density (PMMA) was measured, being $\rho_1=1182$ kg/m^3 (25 °C).

The reflection coefficient was measured using the MRM and RRM methods at the frequency $f_1=1.4$ MHz, the transmitted pulse peak component frequency. The propagation velocity and the density were calculated. Fifteen measurements were taken for each case. The average and standard deviation are presented in Tables II and III. The density results were compared to the measured values of Table I and the deviation

TABLE I. Densities of the liquid samples obtained using a pycnometer (25.0±0.5 °C).

Liquid	Density (kg/m^3)
Distilled water	997.1 ± 0.2
Ethanol (general purpose)	820.4 ± 0.2
Castor oil	956.2 ± 0.2

TABLE II. Experimental results obtained for the MRM method (25.0 ±0.5 °C).

MRM method liquid	Reflection coefficient		Propagation velocity (m/s)		Density (kg/m^3)		
	mean	s.d.	mean	s.d.	mean	s.d.	Δ%
Dist. water	0.361	0.001	1496.4	0.0	1007	1	+1.0
Ethanol	0.520	0.001	1235.9	0.0	820	2	−0.0
Castor oil	0.379	0.001	1502.3	0.0	962	3	+0.6

Δ% is presented. It should be noticed that the propagation velocity was calculated as a function of time delay, which was obtained by cross correlation of sampled data (100-MHz sampling rate). This leads to a resolution of the velocity measurement of about 1 m/s. As the velocity measurement is a discrete process, one can understand the null standard deviation values shown in the tables.

The normalized spectra A_0, A_1, and A_2 of the pulses a_0, a_1, and a_2 are shown in Fig. 8 for the castor oil, which has a large attenuation coefficient. One can observe that higher frequency components are attenuated as the pulse propagates through the sample.

B. Density measurement of flowing liquids

In order to do experiments with flowing liquids, a pipeline with flowing water was built. The flow rate in this line can be controlled with a 1% accuracy in the range of 1–20 ℓ/s. The average fluid velocity in the measurement cell ranges from 0 to 13 m/s (laminar to turbulent with cavitation flow). The liquid temperature is not controlled. The distance between buffer rod II and the reflector was measured to be $L=8.83$ mm. The data were processed as in the previous section, and the results are presented in Tables IV and V. The water density was measured using a pycnometer (24±1 °C), being 997.3±0.3 kg/m^3. These experiments were repeated several times.[12]

It was noticed that when cavitation occurs, the results become inconsistent, so the last measurements in Tables IV and V were discarded. Although some kind of relationship between flow velocity and density may be induced by Tables IV and V, this was not observed in other measurements. The apparent dependence of the propagation velocity on flow velocity may be explained by the variation of the ambient temperature during the experiments in the range of 24±1 °C. The reflection coefficient and the density variation are within the range expected by the precision of the method.

TABLE III. Experimental results obtained for the RRM method (25.0 ±0.5 °C).

RRM method liquid	Reflection coefficient		Propagation velocity (m/s)		Density (kg/m^3)		
	mean	s.d.	mean	s.d.	mean	s.d.	Δ%
Dist. water	0.365	0.001	1496.4	0.0	997	2	−0.0
Ethanol	0.519	0.001	1235.9	0.0	823	2	+0.3
Castor oil	0.381	0.001	1502.3	0.0	957	3	+0.1

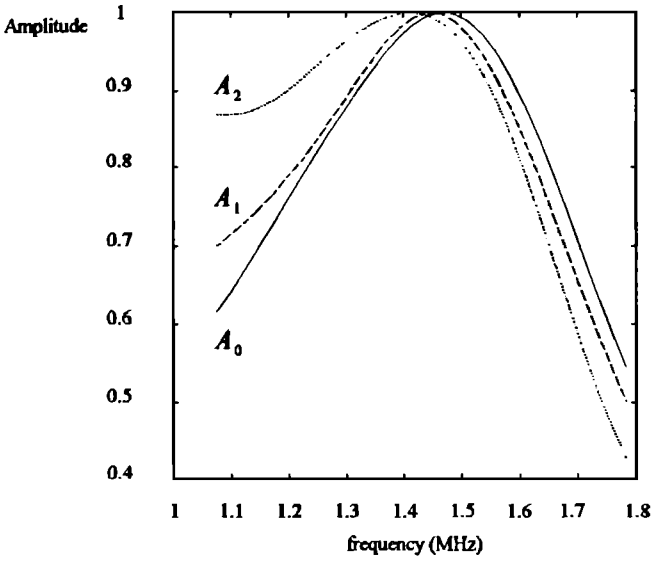

FIG. 8. Normalized spectra of the pulse as it propagates through the castor oil sample.

C. Error analysis

The principal sources of error in the measurement of distilled water density by the MRM method were analyzed and classified into random and systematic errors. A similar analysis of the RRM method leads to analogous results.

In the case of random errors, the digitizing process and the noise contained in the echo signals cause a relative error of about 0.3% on the reflection coefficient measurement (R_{12}). Besides, the time domain discretization causes a relative error of about 0.1% on the sample propagation velocity measurement. By differentiation of Eq. (7) with respect to its variables, one can arrive at the formula for the standard deviation in the sample density, obtaining 0.3% in this case. It can be verified that the standard deviation values experimentally obtained have the same magnitude of the expected value presented.

In relation to the systematic errors, the influence of the system nonlinearities (oscilloscope, amplifiers, etc.) on the reflection coefficient measurement was considered to be typically 1%. The measurement cell assembly guarantees a typical parallelism of 0.001 mm/mm between the buffer rod/sample and the sample/reflector interfaces. In order to verify the influence of the parallelism on the reflection coefficient,

TABLE IV. Results obtained for flowing water for the MRM method (24 ±1 °C).

Mean flow velocity (m/s)	Reflection coefficient		Propagation velocity (m/s)		Density (kg/m³)		
	mean	s.d.	mean	s.d.	mean	s.d.	Δ%
0.0	0.361	0.001	1494.2	0.6	1007	2	+1.0
2.0	0.362	0.001	1493.3	0.0	1006	1	+0.9
4.0	0.362	0.001	1494.6	0.0	1005	1	+0.8
5.8	0.362	0.001	1495.7	0.4	1004	3	+0.7
7.9	0.362	0.002	1497.1	0.0	1003	6	+0.6
10.3[a]	0.369	0.011	1502.3	0.8	983	25	−1.5

[a]Cavitation occurred. This measurement must be discarded.

TABLE V. Results obtained for flowing water for the RRM method (24 ±1 °C).

Mean flow velocity (m/s)	Reflection coefficient		Propagation velocity (m/s)		Density (kg/m³)		
	mean	s.d.	mean	s.d.	mean	s.d.	Δ%
0.0	0.368	0.001	1494.2	0.6	991	2	−0.6
2.0	0.368	0.001	1493.3	0.0	991	3	−0.6
4.0	0.367	0.001	1494.6	0.0	993	1	−0.4
5.8	0.366	0.001	1495.7	0.4	994	2	−0.3
7.9	0.364	0.001	1497.1	0.0	998	2	+0.1
10.3[a]	0.360	0.001	1502.3	0.8	1003	2	+0.6

[a]Cavitation occurred. This measurement must be discarded.

two measurements were conducted in distilled water. Initially, the measurement cell was adjusted to an alignment of 0.0004 mm/mm, which is the best achievable with this assembly, and the reflection coefficient R_{12} was measured. Then a 0.0024-mm/mm misalignment between these interfaces was caused and a 0.7% decrease in the reflection coefficient was observed. From this result, the influence of the interface misalignment on the reflection coefficient was assumed to be less than 0.4% in the experiments presented in this work. The error in the buffer rod density measurement (reference) was estimated to be about 0.1%. The membrane and the adhesive thicknesses had not been considered in the propagation velocity evaluation at the buffer rod, so an error of approximately 0.1% was considered. The error on the reflection coefficient due to diffraction in a measurement cell that uses a standard ceramic transducer in spite of the DET was evaluated using the results presented by Khimunin,[13] being 0.5%. However, this effect is eliminated by using the DET. The maximum systematic error of the density measurement can be obtained by differentiating Eq. (7) with respect to its variables. Considering the worst case, this leads to an estimated accuracy of 1.4%.

Analyzing the experimental results, one can observe that the deviations Δ% experimentally obtained are consistent when compared to the maximum systematic error presented. The previous analysis shows that in order to enhance the density measurement accuracy in the MRM method it would be necessary to reduce the nonlinearity errors and to improve the parallelism between the DET and the reflector interfaces.

VIII. CONCLUSIONS

Two methods to measure the density of liquids (stationary and in motion) were presented. Both methods are based on the measurement of the reflection coefficient at the interface between the liquid sample and a known material (buffer rod II), and the propagation velocity in the liquid sample. The reflection coefficient is measured by two different methods, multiple reflection method and relative reflection method. In the former the reflection coefficient is directly obtained and in the latter a relative measurement is done. Both methods are affected by diffraction effects. In this paper the double-element transducer is introduced in order to eliminate these effects. Besides this, the DET also eliminates the effects of the electronic and the ceramic transducer stability in the RRM method. All the discussion presented in

this work is based on the unidimensional wave propagation model. This is acceptable because of the use of the DET, which is a plane-wave receptor.

In the RRM method, variation in temperature influences the attenuation in buffer rod II and, consequently, the density measurement. By selecting an appropriate buffer rod material and operation frequency, this effect may be neglected in a particular temperature range. Variation in temperature also influences the propagation velocity in the buffer rod and, consequently, the buffer rod impedance and the liquid density measurement. In the methods presented in this paper, this problem was solved by measuring this propagation velocity at each data acquisition.

The propagation velocity is calculated by measuring the time delay between successive echoes, using the cross-correlation method. Although the pulse shape varies along the path due to frequency-dependent attenuation, it is demonstrated in this paper (see Appendix B) that this phenomenon does not affect the measurement of time delay by cross-correlation.

In this work, density measurements of flowing liquids in a wide range of flow rates were conducted. Coherent results were obtained even in turbulent flow, provided that cavitation was not present. From the experimental results, it seems that the measurement is not affected by the flow rate.

It was noticed that the mounting precision of the measurement cell assembly deeply influences the results. The parallelism among the several interfaces must be good enough in order to guarantee normal incidence. The amplitude measurement (analyzed at a particular frequency) is what most influences the density measurement. An accuracy of about 1% was achieved in the density measurement for liquids covering a wide range of densities and attenuations.

For application in large-diameter pipelines, the RRM method becomes more convenient, because in the calculation of the reflection coefficient, only the first pulse (a_0) is needed. However, corrections must be done to compensate for the effects of temperature change on the attenuation coefficient of buffer rod II.

At the moment, a portable real-time measuring instrument is being developed. The system architecture is based on an IBM PC-386 compatible microcomputer board, with a fast data-acquisition board (25 MHz) and a specially designed pulser–receiver board.

ACKNOWLEDGMENTS

The authors would like to thank Finep/PADCT for funding the research program leading to this publication and FAPESP for sponsoring the visit of Professor R. A. Sigelmann to the Universidade de São Paulo. Acknowledgment is made to Dr. Max Gerken, Eng. Ricardo T. Higuti, and Eng. Cacildo B. Palhares, Jr. for their helpful discussions.

APPENDIX A: CALCULATION OF THE IMAGINARY COMPONENT OF THE CHARACTERISTIC (SPECIFIC) ACOUSTIC IMPEDANCE

The complex specific acoustic impedance of a medium is $Z=\rho c_c$, where ρ is the density and c_c is the complex propagation velocity:

$$c_c=\frac{\omega}{\omega/c-j\alpha}=\frac{c}{1-j\alpha c/\omega}, \tag{A1}$$

where c is the real propagation velocity, ω the angular frequency ($\omega=2\pi f$), and α the attenuation coefficient (Np/m). For castor oil[14] the attenuation (α/f^2) is $10\,900\times10^{-15}$ Np/(m Hz^2) (19 °C) and the velocity of propagation is 1500 m/s. Using this data, the ratio between the real and imaginary components ($\alpha c/\omega$) becomes approximately 1/250 at the frequency 1.6 MHz. As castor oil attenuation is in the high end of the liquids that this paper is considering, the imaginary component of the propagation velocity was neglected in this work.

APPENDIX B: ANALYSIS OF THE CROSS-CORRELATION TECHNIQUE

In this Appendix it is shown that the total time delay given by the cross-correlation technique is not affected by attenuation, provided that the ratio between the real and imaginary components of the complex propagation velocity is small enough not to affect the real component (see Appendix A).

A plane and continuous wave that propagates in the z direction through a lossy medium is given by the phasor

$$A=A_0e^{-\alpha(\omega)z}e^{jkz}, \tag{B1}$$

where $\alpha(\omega)$ is the attenuation coefficient, ω the angular frequency, k the wave number, and A_0 the amplitude at $z=0$. The attenuation coefficient α is related to the frequency by the expression[9]

$$\alpha(\omega)=\alpha_0\omega^n, \tag{B2}$$

where $0.5<n\leq2$ and α_0 is real. Notice that $\alpha(\omega)$ is always real.

Let $a_i(t)$ be the first echo (reference) and $a_j(t)$ the second echo, then,

$$a_j(t)=Ka_i(t)*\delta(t-D/c)*g(t), \tag{B3}$$

where K is a constant, $\delta(t)$ the Dirac function, D the distance traveled by the wave in the lossy medium, c the propagation velocity in this medium, $g(t)$ the effect due to attenuation, and * the convolution operation. The term $\delta(t-D/c)$ represents the total time delay due to the propagation.

The cross correlation $\gamma_{a_ia_j}(t)$ of $a_i(t)$ and $a_j(t)$ is

$$\begin{aligned}\gamma_{a_ia_j}(t)&=a_i(t)\oplus a_j(t)=a_i(-t)*a_j(t)\\&=a_i(-t)*Ka_i(t)*\delta(t-D/c)*g(t),\end{aligned} \tag{B4}$$

where $\oplus$ is the cross-correlation operation. In order to discover when the maximum of $\gamma_{a_ia_j}(t)$ occurs, first it will be shown that the absolute maximum of the function

$$f(t)=a_1(-t)*a_i(t)*g(t) \tag{B5}$$

occurs at $t=0$.

The autocorrelation of the signal $a_i(t)$ is

$$\gamma_{a_ia_i}(t)=a_i(t)\oplus a_i(t)=a_i(-t)*a_i(t), \tag{B6}$$

and its Fourier transform $\Gamma_{a_ia_i}(\omega)$ is

$$\Gamma_{a_i a_i}(\omega)=A_i^*(\omega)A_i(\omega), \tag{B7}$$

where $A_i(\omega)$ is the Fourier transform of $a_i(t)$, and $A_i^*(\omega)$ is its complex conjugate. Notice that $\Gamma_{a_i a_i}(\omega)$ is real and positive for any ω. The attenuation function $G(\omega)$ may be written as

$$G(\omega)=e^{-\alpha(\omega)D}, \tag{B8}$$

where $G(\omega)$ is the Fourier transform of $g(t)$. As $\alpha(\omega)$ is real, $G(\omega)$ is real and positive for any ω. From Eq. (B5),

$$F(\omega)=\Gamma_{a_i a_i}(\omega)G(\omega), \tag{B9}$$

where $F(\omega)$ is the Fourier transform of $f(t)$, and $F(\omega)$ is real and positive for any ω. But $f(t)$ is given by

$$f(t)=\frac{1}{2\pi}\int_{-\infty}^{\infty}F(\omega)e^{j\omega t}\,d\omega, \tag{B10}$$

and

$$f(0)=\frac{1}{2\pi}\int_{-\infty}^{\infty}F(\omega)d\omega. \tag{B11}$$

As $F(\omega)$ is real and positive for any ω, the following inequality may be written

$$\left|\frac{1}{2\pi}\int_{-\infty}^{\infty}F(\omega)e^{j\omega t}\,d\omega\right|_{t\neq 0}<\frac{1}{2\pi}\int_{-\infty}^{\infty}F(\omega)d\omega. \tag{B12}$$

Then

$$|f(t)|_{t\neq 0}<f(0), \quad \text{for any } t,\ t\neq 0; \tag{B13}$$

thus $f(0)$ is the maximum of the function $f(t)$.

From Eq. (B4), the maximum of $\gamma_{a_i a_j}(t)$ occurs at $t=D/c$, because

$$\gamma_{a_i a_j}(t)=K\delta(t-D/c)*f(t). \tag{B14}$$

Hence, if the attenuation function is of the form of Eq. (B8) and the imaginary component of the propagation velocity is negligible ($\alpha c/\omega \ll 1$), the time delay between two echoes obtained by the cross-correlation technique is not affected by the attenuation.

[1] J. M. Hale, "Ultrasonic density measurement for process control," Ultrasonics **26**, 356–357 (1988).

[2] D. J. McClements and P. Fairley, "Ultrasonic pulse-echo reflectometer," Ultrasonics **29**, 58–62 (1991).

[3] E. P. Papadakis, K. A. Fowler, and L. C. Lynnworth, "Ultrasonic attenuation by spectrum analysis of pulses in buffer rods: Method and diffraction corrections," J. Acoust. Soc. Am. **53**, 1336–1343 (1973).

[4] E. P. Papadakis, "Buffer-rod system for ultrasonic attenuation measurements," J. Acoust. Soc. Am. **44**, 1437–1441 (1968).

[5] E. P. Papadakis, "Absolute measurements of ultrasonic attenuation using damped nondestructive testing transducers," J. Test. Eval. **12**, 273–279 (1984).

[6] B. Klime, "System and method for ultrasonic determination of density," U.S. Patent No. 4,991,124 (1991).

[7] J. P. Weight, "Ultrasonic beam structures in fluid media," J. Acoust. Soc. Am. **76**, 1184–1191 (1984).

[8] S. Leeman, D. A. Seggie, L. A. Ferrari, P. V. Sankar, and M. Doherty, "Diffraction-free attenuation estimation," in *Proceedings of Ultrasonic International*, 2–4 July 1985, London (Butterworth, Guildford, U.K., 1985), Vol. 85, pp. 128–132.

[9] E. T. Costa, "Development and application of a large-aperture PVDF hydrophone for measurement of non-linear ultrasound fields," Ph.D. thesis, School of Medicine and Dentistry, King's College at London, 1989.

[10] C. Yeh, "Reflection and transmission of sound waves by a moving fluid layer," J. Acoust. Soc. Am. **41**, 817–821 (1967).

[11] C. C. Habeger and W. A. Wink, "Development of a double-element pulse-echo, PVDF transducer," Ultrasonics **28**, 52–54 (1990).

[12] J. C. Adamowski, "Ultrasonic measurement of density of liquids," Ph.D. thesis, Escola Politécnica da Universidade de São Paulo (1993) (in Portuguese).

[13] A. S. Khimunin, "Numerical calculation of the diffraction corrections for the precise measurement of ultrasound absorption," Acustica **27**, 173–181 (1972).

[14] G. W. C. Kaye and T. H. Laby, *Tables of Physical and Chemical Constants* (Longmann, London, 1973), 14th ed.